Effects of an Elastic Mass on Frequency Response Characteristics of an Ultra-Thin Piezoelectric Micro-Acoustic Actuator

Hye Jin Kim, Woo Seok Yang, and Kwangsoo No

***Abstract*—This paper presents an optimized method to improve the sound quality of ultra-thin piezoelectric micro-acoustic actuators. To achieve flat and smooth frequency response characteristics of the piezoelectric acoustic actuators, we have proposed an elastic mass attached to the acoustic diaphragm. The effects of the elastic mass on frequency response characteristics of the piezoelectric acoustic actuator were investigated by finite element analysis simulation and laser scanning vibrometer measurement. Based on the modal and vibrational characteristics, it was found that the fabricated piezoelectric acoustic actuator has a significant dip of 1.32 kHz and peak of 2.24 kHz, which correspond respectively to the (1,3) and (3,1) resonant modes of the acoustic diaphragm. However, by attaching an elastic mass to the acoustic diaphragm with a shape similar to the (3,1) mode, the resonant frequencies corresponding to the (1,3) and (3,1) modes shifted to higher frequencies and the vibrational displacements at each mode were dramatically reduced by about 40%. As a result, the dip at (1,3) mode was greatly improved by 13 dB and total harmonic distortion was dramatically reduced from 80.83% to 8.71%. This paper shows that the optimized elastic mass can allow flat and smooth frequency response characteristics by improving the significant peak and dip.**

I. Introduction

Piezoelectric ceramic materials have been widely used in many applications, such as piezoelectric sensors and actuators. Piezoelectric sensors are devices that use the direct piezoelectric effect to measure external mechanical force, pressure, or strain by converting them to an electrical charge. They have been successfully used in piezoelectric microphones, pressure sensors, piezoelectric accelerometers, ultrasonic sensors, etc. Piezoelectric actuators are devices that use the inverse piezoelectric effect, which generates a mechanical strain resulting from an applied electrical field. Their applications include piezoelectric acoustic actuators, valves, pumps, motors, ink-jet print heads, ultrasonic motors, laser scanners, etc. [1]–[5].

Manuscript received February 1, 2013; accepted May 13, 2013. This work was supported by the IT R&D programs of the Ministry of Knowledge Economy (MKE)/Korea Evaluation Institute of Industrial Technology (KEIT) [Development of self-powered smart sensor node platform for smart & green building (10035570) and Development of multilayer piezoelectric ceramic based low-voltage driving thin speaker (10038786)] and MKE/INNOPOLIS [Development technologies of piezoelectric ceramic speaker with low driving voltage, thin thickness and enhanced low frequency sound for mobile applications].

H. J. Kim and W. S. Yang are with the Electronics and Telecommunications Research Institute, Daejeon, Korea (e-mail: nolawara@etri.re.kr).

K. No is with the Department of Material Science and Engineering, KAIST, Daejeon, Korea.

DOI http://dx.doi.org/10.1109/TUFFC.2013.2739

The piezoelectric acoustic actuator (usually called a piezoelectric ceramic speaker) is a piezoelectric actuator that produces sound in response to an electrical audio signal input by the inverse piezoelectric effect. Recently, ultra-thin piezoelectric acoustic actuators have attracted a great deal of attention for ultra-slim portable electronic devices such as smartphones and tablet PCs, as the most promising alternatives to overcome the thickness limitation of traditional dynamic speakers. To date, ultra-thin piezoelectric acoustic actuators have been developed using various piezoelectric materials such as AlN, lead zirconate titanate [$Pb(Zr_x,Ti_{1-x})O_3$; PZT], lead magnesium niobate–lead titanate [$(1-x)Pb(Mg_{1/3}Nb_{2/3})O_3$-$xPbTiO_3$; PMN-PT], and so on [6]–[14].

Yi *et al.* proposed an ultra-thin AlN piezoelectric microspeaker with a high acoustic output performance by implementing a package structure with the AlN film [6]. They showed that the output sound pressure of the fabricated ultra-thin piezoelectric microspeaker was enhanced by more than 10 dB with a higher compressively stressed composite diaphragm at a low- to medium-frequency range. Cho *et al.* provided a piezoelectric microspeaker with large sound pressure level comparable to a commercial piezoceramic speaker despite its smaller form factor [7]. They reported the piezoelectric microspeaker fabricated on a diaphragm of only 5 × 5 mm with highly c-axis oriented ZnO thin film on a heavily compressive-stressed silicon-nitride film. They also observed that the sound pressure of the small and thin piezoelectric microspeaker was about 92 dB at a distance of 3 mm under input voltage of 6 V_{pp}, which was nearly the same as that of a commercial piezoceramic speaker. Kim *et al.* presented high-performance PMN-PT single-crystal piezoelectric microspeakers fabricated using silicon-based microelectromechanical systems (MEMS) technology [8]. They reported that the fabricated PMN-PT piezoelectric speakers had a thickness of just 0.5 mm and an area of just 1.5 × 1.5 cm and output sound pressure levels of about 85 dB at a distance of 1 cm with an input drive of 14 V_{pk}, which produces a competitive output compared with other commercial piezoelectric microspeakers. They also demonstrated an improved PZT piezoelectric microspeaker with a high sound pressure level of 90 dB at a distance of 10 cm under input voltage of 16 V_{pk} [9]. The fabricated PZT ceramic microspeaker had a thickness of only 1 mm, including the speaker frame. They discussed the enhancement of the output sound pressure of the ultra-thin PZT piezoelectric microspeaker at a low-frequency range by the silicone buf-

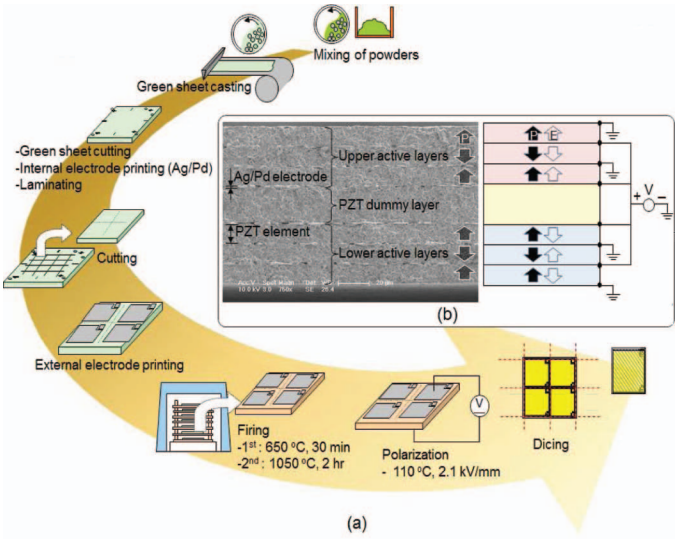

Fig. 1. (a) The fabrication processes and (b) the cross-sectional field emission scanning electron microscope (FE-SEM) image of the triple-layered piezoelectric multimorph ceramic sheet. Herein, P and E indicate the polarization direction and the applied electric field in each piezoelectric active layer, respectively.

fer layer, which offers performance competitive with other commercial piezoelectric microspeakers of the same size.

These piezoelectric ceramic speakers have several obvious benefits of being thinner, more power-efficient, and lighter than traditional dynamic speakers. However, most of these piezoelectric ceramic speakers have suffered from bad sound playback quality because of their irregular jagged frequency response characteristics. Typically, the traditional moving-coil speakers have good sound quality over a wide playing range because of the pistonic motions of their acoustic diaphragms. In contrast, the acoustic diaphragms of piezoelectric ceramic speakers vibrate with many resonant modes, which lead to acoustic peaks and dips in their irregular jagged frequency response characteristics. Because of these acoustic peaks and dips, the sound quality of the piezoelectric acoustic actuators is usually worse than traditional moving-coil speakers [15]. The bad sound quality is an important shortcoming that has restricted the expansion of the commercialization of the piezoelectric acoustic actuators.

To date, there have been several reports on improving the sound quality of the piezoelectric acoustic actuators [15]–[17]. They have mainly focused on the theoretical and experimental results based on the distributed-mode motions of the loudspeakers. However, most of these reports have used piezoelectric loudspeakers with large acoustic diaphragms which are not suitable for alternatives to the traditional dynamic speakers being used in portable devices. In this paper, we introduce an ultra-thin piezoelectric micro-acoustic actuator for mobile terminals and investigate the vibrational frequency response characteristics based on an elastic mass attached to the acoustic diaphragm to improve the acoustic performance. To investigate the vibrational frequency response characteristics of the piezoelectric acoustic actuator, we simulated and analyzed the modal vibration characteristics of the acoustic diaphragm using finite-element analysis (FEA) and laser scanning vibrometer (LSV) measurement, respectively. This paper presents the effects of the elastic mass on the sound quality of the piezoelectric micro-acoustic actuator.

II. Fabrication of the Piezoelectric Acoustic Actuators

Generally, the piezoelectric acoustic actuators are comprised of an acoustic diaphragm fixed to a rigid frame and a piezoelectric ceramic membrane bonded on the acoustic diaphragm.

First, the Nb-doped PZT [$Pb(Zr_{0.56},Ti_{0.44})O_3$] piezoelectric ceramic sheets were prepared to have the triple-layered parallel multimorph structure; they are composed of three piezoelectric layers: the upper and lower piezoelectric active layers and the piezoelectric dummy layer. Fig. 1 shows the fabrication processes and the cross-sectional field emission scanning electron microscope (FE-SEM) image of the triple-layered piezoelectric multimorph ceramic sheet.

The piezoelectric green sheets were prepared by tape casting using commercial powders (PbO, ZrO_2, TiO_2, and Nb_2O_5) and then 1-μm-thick Ag/Pd pastes were printed on the green sheets as internal electrodes. These printed sheets were stacked, pressed, and dried for lamination. After the laminating and cutting process of the green sheets, all of the green chips were printed with the external electrodes and sintered. The sintering process included two major firing stages: the first step to burn out all the organic components of the screen-printed ceramics at 650°C for 30 min and a sintering step to densify the ceramics at 1050°C for 2 h. Then, the sintered PZT ceramics were polarized under an electric field of 2.1 kV/mm at 110°C for 3 min. Finally, the PZT piezoelectric ceramics were completed by the Au plating and dicing process. Herein, the parallel triple-layered multimorph piezoelectric ceramics were electrically connected in parallel because the parallel connection can provide much larger deformation than the series connection for the same electric voltage applied [5], [18]. In other words, the electric fields for the upper active layer are applied in the direction of the polarization but those for the lower active layer are applied in the opposite direction of the polarization, as shown in Fig. 1(b). Thus, the piezoelectric constitutive equations for each upper and lower active layer of the fabricated piezoelectric ceramics can be written as follows [18]–[20]:

$$\begin{aligned} S_1^{\mathrm{U}} &= s_{11}^{\mathrm{E}} T_1^{\mathrm{U}} + d_{31} E_3^{\mathrm{U}} \\ D_3^{\mathrm{U}} &= \varepsilon_{33}^{\mathrm{T}} E_3^{\mathrm{U}} + d_{31} T_1^{\mathrm{U}} \\ S_1^{\mathrm{L}} &= s_{11}^{\mathrm{E}} T_1^{\mathrm{L}} - d_{31} E_3^{\mathrm{L}} \\ -D_3^{\mathrm{L}} &= -\varepsilon_{33}^{\mathrm{T}} E_3^{\mathrm{L}} + d_{31} T_1^{\mathrm{L}}, \end{aligned} \tag{1}$$

where S_1 and T_1 are the mechanical strain and stress vectors in the length direction of the piezoelectric elements;

D_3 and E_3 are the electric displacement and electric field vectors; and s_{11}^{E}, $\varepsilon_{33}^{\mathrm{T}}$, and d_{31} are the elastic compliance at constant electric field, dielectric permittivity tensor at constant stress, and transverse piezoelectric coefficient, respectively. These constitutive equations indicate that the parallel triple-layered multimorph ceramics in parallel connection result, respectively, in shrinkage and expansion at the upper and lower active layers with the applied electric field. As a result, the electrical parallel connection of the fabricated parallel multimorph ceramics can provide large bending deformation so that they generate much larger displacements compared with the series connection. The fabricated piezoelectric ceramic sheets had dimension of 17 × 11 mm and total thickness of 110 μm. The thicknesses of each piezoelectric element in the active layers and the dummy layer of the fabricated ceramic were 13 and 25 μm, respectively.

Next, the fabricated piezoelectric ceramic sheets were bonded onto the acoustic diaphragms, which are made from a rubber/resin bi-layer diaphragm. The used rubber/resin bi-layer acoustic diaphragm consisted of a 100-μm-thick silicone rubber layer and 50-μm-thick polyprophylene (PP) resin film. Here, the rubber/resin bi-layer film had the dimensions of 15 × 20 mm and 13 × 18 mm, respectively, to make the acoustic diaphragm more flexible so the flexible acoustic diaphragm can enhance the output acoustic characteristics of the piezoelectric acoustic actuators at the low-frequency range [5]. As a result, the total dimensions and thickness of the flexible acoustic diaphragm fabricated by rubber/resin bi-layer film were 15 × 20 mm and 150 μm, respectively.

Finally, the acoustic diaphragm bonded with the parallel triple-layered multimorph piezoelectric ceramic sheet was fixed to a rigid printed circuit board (PCB) frame, and electrically connected to terminals. The total dimension and thickness of the fabricated ultra-thin piezoelectric micro-acoustic actuator were only 23.5 × 17 mm and 0.8 mm, respectively.

III. Results and Discussion

A. Frequency Response Characteristics

Typically, unlike the traditional dynamic speakers, the piezoelectric acoustic actuators vibrate with many resonant modes which lead to acoustic peaks and dips in the jagged sound pressure level (SPL). Above all, several serious peaks and dips in the frequency response characteristics can degrade the sound quality of the piezoelectric acoustic actuator, resulting in higher total harmonic distortion (THD) characteristics. The percentage of THD can be defined by [9]

$$\%\mathrm{THD} = 100 \times \sqrt{\frac{A_2^2 + A_3^2 + \cdots + A_N^2}{A_1^2 + A_2^2 + A_3^2 + \cdots + A_N^2}}, \quad (2)$$

where terms 2 to N are the power levels (A_2^2 to A_N^2) of the harmonics, and term 1 is the power level (A_1^2) of the fundamental (pure) tone. Herein, As are the amplitudes of the fundamental and harmonic components. According to (2), it is obvious that higher THD characteristics generated by higher order nonlinear harmonics lead to worse sound quality of the fabricated piezoelectric micro-acoustic actuator. Hence, reducing the significant peaks and dips in the jagged sound pressure characteristics improves the sound quality of the piezoelectric acoustic actuator by reducing the harmonic distortion in the audible frequency range.

To investigate the relation between the peaks and dips in the frequency response characteristics and the sound quality of the piezoelectric acoustic actuator, we measured and analyzed the acoustic frequency response characteristics of the fabricated piezoelectric acoustic actuator. Fig. 2 shows the measured output sound pressure and THD characteristics of the fabricated piezoelectric micro-acoustic actuators. The output SPL and THD characteristics of the fabricated piezoelectric acoustic actuator were measured with an input drive voltage of 14 V_{pk} using a B&K 3560 pulse analyzer (Brüel & Kjær AS, Nærum, Denmark), and obtained by the 4191 1/2-in (12.7-mm) reference microphone at a distance 10 cm away from the exits of the speaker. For measurement, the fabricated piezoelectric acoustic actuator was fixed to a baffle plate of 50 × 50 cm.

As shown in Fig. 2(a), the fabricated piezoelectric micro-acoustic actuator vibrates with many peaks and dips in the jagged frequency response characteristics. For an ideal piezoelectric ceramic speaker, it can be modeled by the single-resonance system, for which the output sound pressure level is approximately independent of the frequency above the fundamental resonant frequency, but is proportional to the square of frequency below it [5], [11], [21]. Hence, it is obvious that the first peak of 280 Hz is the fundamental resonant frequency of the fabricated piezoelectric ceramic speaker. However, the output sound pressure of the fabricated piezoelectric acoustic actuator fluctuates depending on the frequency, unlike the model of the ideal piezoelectric speaker. Especially, the fabricated piezoelectric micro-acoustic actuator has a significant dip of 1.32 kHz and peak of 2.24 kHz, which correspond to higher harmonic distortion characteristics shown in Fig. 2(b). The measured THDs at 1.32 and 2.24 kHz are 80.83% and 8.15%, respectively. This result means that the serious peak and dip in the frequency response can degrade the sound quality of the piezoelectric ceramic speaker by the increased harmonic distortion.

Meanwhile, it was already shown that the first peak of 280 Hz in the jagged frequency response corresponds to the fundamental resonant frequency of the fabricated piezoelectric acoustic actuator. This result indicates that the peaks and dips in the jagged frequency response depend on the resonant frequencies of the fabricated piezoelectric acoustic actuator. To verify the dependence of

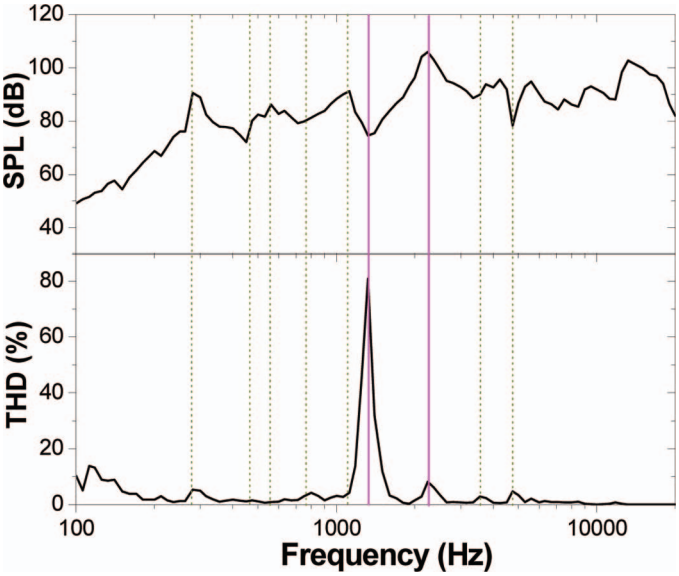

Fig. 2. The measured output sound pressure level (SPL) and total harmonic distortion (THD) characteristics of the fabricated piezoelectric micro-acoustic actuator.

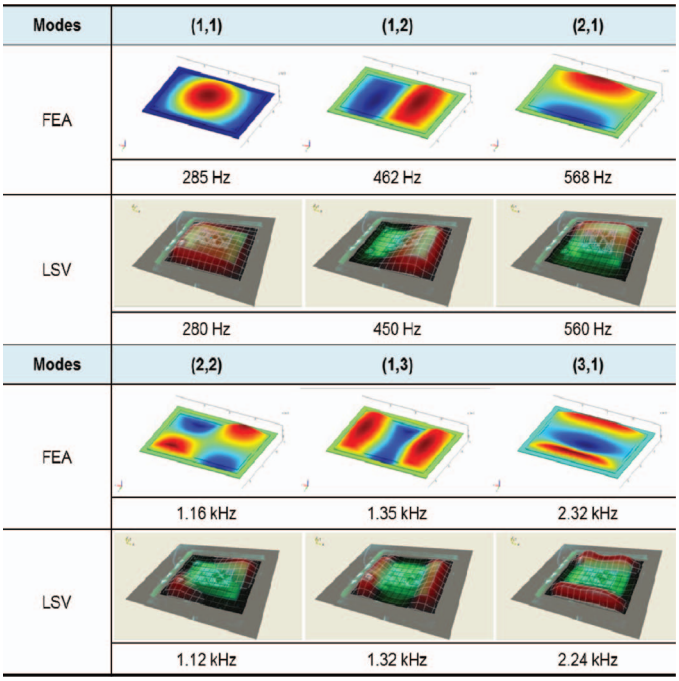

Fig. 3. The simulated and measured vibrational mode shapes and resonant frequencies of the fabricated piezoelectric micro-acoustic actuator.

the acoustic peaks and dips in the frequency response on the resonant frequencies of the piezoelectric acoustic actuator, we simulated and analyzed the vibrational modal and displacement characteristics of the fabricated piezoelectric speaker using Comsol Multiphysics (Comsol Inc., Burlington, MA) FEA method and LSV measurement, respectively. Figs. 3 and 4 show the simulated and measured vibrational mode shapes and the average vibrational displacement spectrum of the fabricated piezoelectric acoustic actuator, respectively. The average vibrational displacement characteristics were measured with an input drive voltage of 5 V_{pk} using a Polytec PSV400 laser scanning vibrometer (Polytec GmbH, Waldbron, Germany).

As shown in Fig. 3, the simulated modal characteristics are in good agreement with the LSV measurement results. For example, the simulated fundamental resonant frequency of the fabricated piezoelectric acoustic actuator was about 285 Hz. Similarly, the measured fundamental resonant frequency was 280 Hz. These results confirm that the first peak of 280 Hz in the frequency response shown in Fig. 2 is the fundamental resonant frequency of the fabricated piezoelectric acoustic actuator. Moreover, from Figs. 3 and 4, it is shown that the simulated and measured resonant modes of the fabricated piezoelectric acoustic actuator correspond to the acoustic peaks and dips in the jagged frequency response characteristics.

As shown in Fig. 4, the fabricated piezoelectric micro-acoustic actuator has a significant dip of 1.32 kHz and a peak of 2.24 kHz which correspond respectively to the (1,3) and (3,1) modes of the acoustic diaphragm. The serious dip and peak obviously result in the bad sound quality of the fabricated piezoelectric acoustic actuator, as described in Fig. 2. Hence, to improve the sound quality of the piezoelectric acoustic actuator, the vibrational characteristics at the (1,3) and (3,1) modes should be improved to achieve flat and smooth frequency response characteristics.

B. Effect of Elastic Mass on Frequency Response Characteristics

This paper presents an optimized method to improve the vibrational characteristics at the (1,3) and (3,1) modes, which correspond to the significant dip and peak

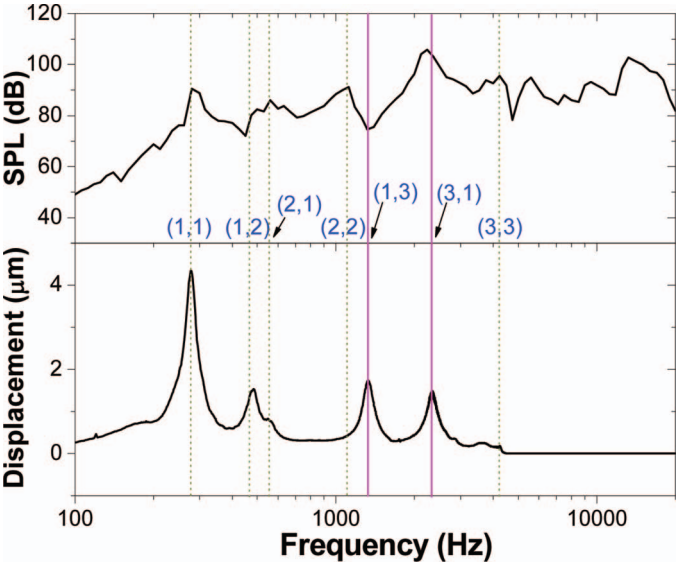

Fig. 4. The measured output sound pressure level and average displacement characteristics of the fabricated piezoelectric micro-acoustic actuator.

in the SPL of the fabricated piezoelectric micro-acoustic actuator. To achieve a smooth and flat sound pressure of the piezoelectric micro-acoustic actuator, we have proposed an elastic mass attached to the acoustic diaphragm, as shown in Fig. 5. The elastic mass used in this paper can effectively control the resonant vibration of the frequency response characteristics and to reduce the significant dip and peak, by enhancing the damping of the acoustic diaphragm, in other words, by acting as a passive damping element [22]–[24]. We attached the prepared elastic mass, with a shape similar to the (3,1) mode, to the acoustic diaphragm using a silicone adhesive (Silicone RTV 9186L, Dow Corning Inc., Midland, MI). Fig. 5 shows the schematic view and photos of the fabricated ultra-thin piezoelectric acoustic actuator before and after attaching the elastic mass. The used elastic mass was an acryl foam material which has the dimension of 4 × 13 mm and thickness of 0.2 mm.

Fig. 6 shows the impedance-phase and capacitance characteristics of the fabricated piezoelectric micro-acoustic actuator before and after attaching the elastic mass to the acoustic diaphragm. All the impedance-phase and capacitance characteristics were measured under the oscillating voltages of 0.1 V_{pk} using an HP-4194A impedance/gain-phase analyzer (Agilent Technology Inc., Santa Clara, CA). The measured impedance and capacitance characteristics provide the in-plane (parallel to the acoustic diaphragm) vibrational modes of the fabricated piezoelectric speakers. As shown in Fig. 6, the measured resonant frequencies of the fabricated piezoelectric acoustic actuator before attaching the elastic mass were in excellent agreement with the simulated and measured vibrational modes shown in Figs. 3 and 4. In other words, the in-plane vibrational modes are observed at the same resonant frequencies with the out-of-plane vibrational modes obtained by LSV measurement. However, after attaching the elastic mass to the vibrational diaphragm, the resonant frequencies which correspond to the (2,2), (1,3), and (3,1) modes, quite shifted from 1.12, 1.32, and 2.24 kHz to higher frequencies of 1.5, 1.66, and 2.68 kHz, respectively. These results can be explained by the fact that the elastic mass attached to the acoustic diaphragm has the same shape as the (3,1) mode so that can purposely disturb the vibrations at (2,2) and (1,3) modes by stiffening the acoustic diaphragm at those modes. Also, these (2,2) and (1,3) resonant modes shifted to higher frequencies by the elastic mass interact with other surrounding modes. Thus, it is evident that the resonant modes shifted by the attached elastic mass strongly influence the vibrational characteristics of the piezoelectric acoustic diaphragm.

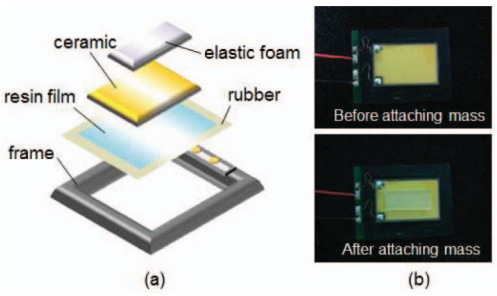

Fig. 5. (a) The schematic view and (b) photos of the fabricated ultra-thin piezoelectric micro-acoustic actuator before and after attaching the elastic mass.

To verify the effect to the elastic mass on the vibrational frequency response characteristics of the fabricated piezoelectric acoustic actuator, we compared the modal and vibrational displacement characteristics before and after attaching the elastic mass to the acoustic diaphragm. Fig. 7 shows the average displacement characteristics of the fabricated piezoelectric micro-acoustic actuator before and after attaching the elastic mass to the acoustic diaphragm and decreasing ratio (β/α) of the displacement characteristics at each resonant mode. And Table I lists the simulated and measured resonant frequencies of the piezoelectric micro-acoustic actuator before and after attaching the elastic mass to the acoustic diaphragm. As shown in Fig. 7, the vibrational displacements at modes below the (3,3) mode were decreased by the elastic mass attached to the acoustic diaphragm. Especially, the vibrational displacements at the (1,3) and (3,1) modes were dramatically reduced, compared with other resonant modes. As shown in Fig. 7(b), the decreasing ratios of the vibrational displacements at other resonant modes except the (1,3) and (3,1) modes are over 0.6, of which the lost performances are acceptable. In contrast, the vibrational displacements at the (1,3) and (3,1) modes were significantly reduced from 1.72 μm to 0.65 μm and from 1.45 μm to 0.65 μm, respectively, by attaching the elastic mass to the acoustic diaphragm. In other words, the decreasing ratios (β/α) of the displacements at the (1,3) and (3,1) modes were respectively 0.38 and 0.44. This result means that the acoustic diaphragm becomes stiffer at the (1,3) and (3,1) modes than other resonant modes, because of the attached elastic mass. In other words, the elastic mass attached to the acoustic diaphragm can selectively reduce the vibrational displacements at each mode by stiffening the acoustic diaphragm.

In common with the results from Figs. 6 and 7, Table I shows that the resonant frequencies at the (2,2), (1,3) and (3,1) modes were quite shifted from 1.12, 1.31, and 2.24 kHz to higher frequencies of 1.5, 1.66, and 2.68 kHz, respectively, by attaching the elastic mass. The simulated resonant frequencies at each mode were also in good agreement with the LSV measurement results. On the other hand, the resonant frequencies at other surrounding modes except the (2,2), (1,3), and (3,1) modes were hardly shifted, as shown in Fig. 7 and Table I. These results are due to the fact that the elastic mass attached to the acoustic diaphragm is similar to the (3,1) mode shape so that it purposely disturbs the vibrations at the (2,2) and (1,3) modes. In addition, the resonance shift of the (3,1) mode can be explained by the fact that the acoustic diaphragm was quite stiffened by the attached elastic mass shape at that mode. In this paper, the vibrational modes and displacement characteristics at a higher fre-

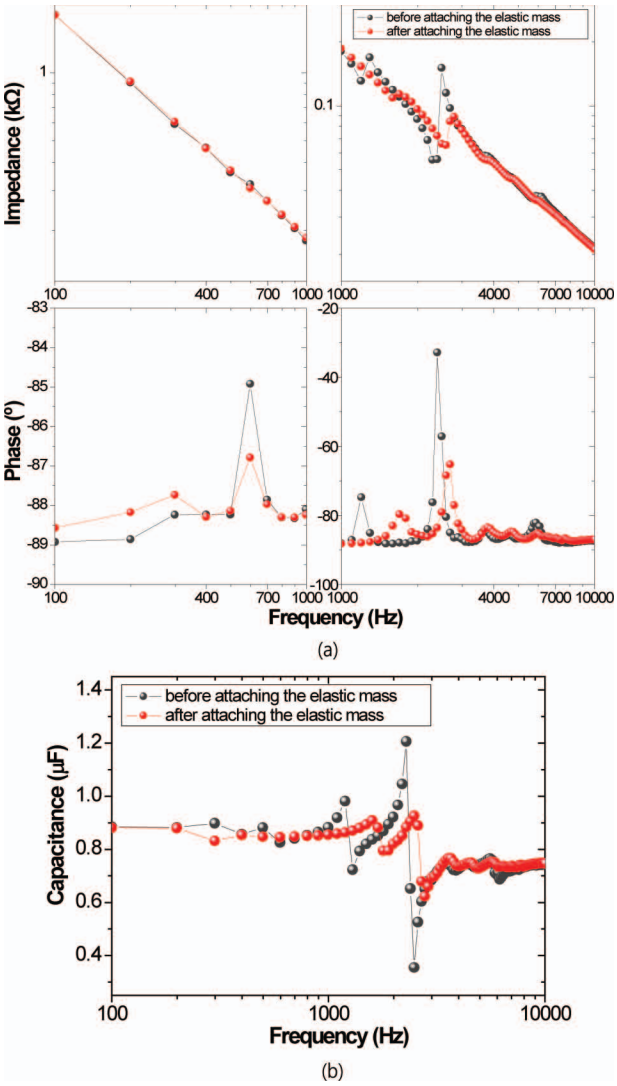

Fig. 6. (a) The impedance-phase and (b) capacitance characteristics of the fabricated piezoelectric micro-acoustic actuator before and after attaching the elastic mass to the acoustic diaphragm.

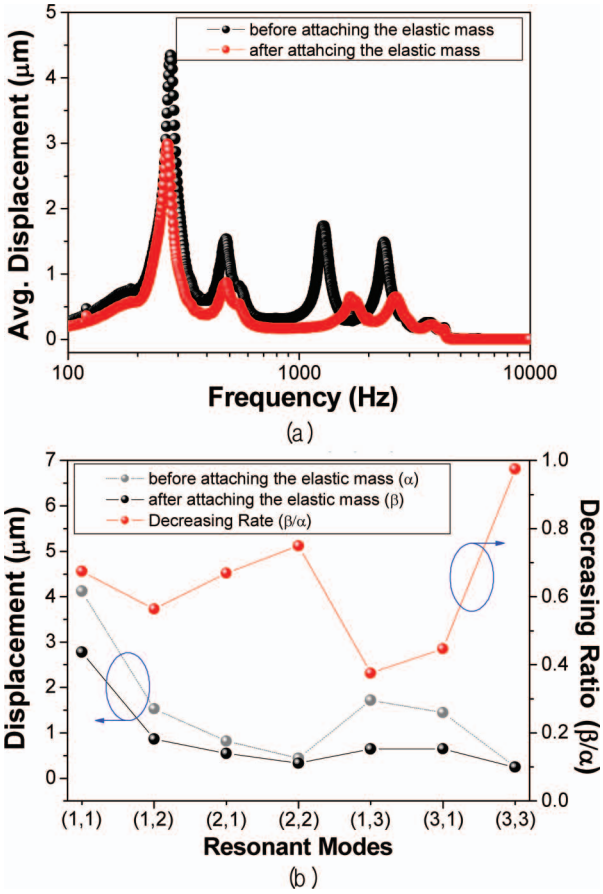

Fig. 7. (a) The measured average displacement characteristics of the fabricated piezoelectric micro-acoustic actuator before and after attaching the elastic mass to the acoustic diaphragm and (b) decreasing ratio (β/α) of the displacement characteristics at each resonant mode.

quency range of the fabricated piezoelectric acoustic actuator were not considered because they obviously have much smaller displacement than the frequency response characteristics at a low- to medium-frequency range, as shown in Fig. 7.

As a result, it is obvious that the attached elastic mass greatly influences on the vibrational characteristics of the fabricated piezoelectric micro-acoustic actuator. At the (2,2), (1,3), and (3,1) modes, the elastic mass attached to the acoustic diaphragm shifted the resonant frequencies to higher values and remarkably reduced the displacement performance. Furthermore, it can be said that the elastic mass attached to the acoustic diaphragm can also reduce the significant peak and dip in sound pressure of

TABLE I. THE SIMULATED (SIM.) AND MEASURED (MEAS.) RESONANT FREQUENCIES OF THE PIEZOELECTRIC ACOUSTIC ACTUATOR BEFORE AND AFTER ATTACHING THE ELASTIC MASS TO THE ACOUSTIC DIAPHRAGM.

	Resonant frequencies (kHz)			
	Before attaching the elastic mass		After attaching the elastic mass	
Mode	Sim.	Meas.	Sim.	Meas.
(1,1)	0.29	0.28	0.3	0.28
(1,2)	0.46	0.45	0.48	0.46
(2,1)	0.57	0.56	0.59	0.56
(2,2)	1.16	1.12	1.56	1.5
(1,3)	1.35	1.32	1.7	1.66
(3,1)	2.32	2.24	2.83	2.68
(3,3)	3.43	3.35	3.51	3.42

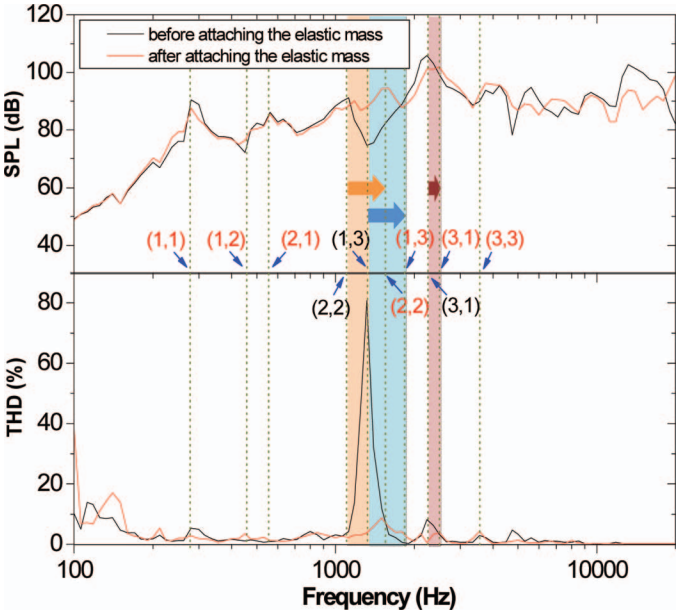

Fig. 8. The output sound pressure levels and total harmonic distortion characteristics of the fabricated piezoelectric micro-acoustic actuator before and after attaching the elastic mass.

the piezoelectric acoustic actuator, to enhance the acoustic frequency response characteristics.

Fig. 8 shows the measured output sound pressure level and THD characteristics of the fabricated piezoelectric micro-acoustic actuator before and after attaching the elastic mass. As shown in Fig. 8, it is obvious that the significant dip in SPL and high THD result of the piezoelectric acoustic actuator are dramatically improved by the elastic mass attached to the acoustic diaphragm. This result is because the (2,2) and (1,3) modes shift to higher frequencies, as shown in Figs. 7 and 8, and interact with other surrounding modes. In other words, the sound outputs and playback quality of the fabricated piezoelectric acoustic actuator can be improved by the elastic mass attached to the acoustic diaphragm. As shown in Fig. 8, by the attached elastic mass, the dip at the (1,3) mode of 1.32 kHz was greatly improved by 13 dB so that the piezoelectric acoustic actuator can have flat and smooth frequency response characteristics. Moreover, the percentage of THD at the (1,3) mode of 1.32 kHz was dramatically reduced from 80.83% to 8.71%. Herein, there is no denying that the output sound pressure of the piezoelectric acoustic actuator at a low-frequency range are also reduced by the attached elastic mass because of the reduced vibrational displacement characteristics shown in Fig. 7. From Fig. 8, the output sound pressure levels at a low-frequency range of less than 1 kHz were reduced by about 3 dB, by attaching the elastic mass to the acoustic diaphragm. As a result, the fabricated piezoelectric acoustic actuator has an average SPL of 85 dB at 10 cm and low THD characteristics of less than 8.7%. These results indicate that the optimized elastic mass allows smooth and flat frequency response characteristics for the improved sound quality of the piezoelectric acoustic actuator.

IV. Conclusions

This paper reports an optimized method to improve the sound quality of the piezoelectric micro-acoustic actuator. Based on modal and vibrational frequency response characteristics of the piezoelectric micro-acoustic actuator, it was shown that the elastic mass attached to the acoustic diaphragm selectively shifts resonant modes which correspond to the significant peak and dip to higher frequencies and remarkably reduces the vibrational displacements at each mode. Moreover, based on the vibrational frequency response characteristics, it was also shown that the significant dip in SPL and high THD result of the piezoelectric acoustic actuator were dramatically improved by the elastic mass attached to the acoustic diaphragm. Hence, it can be concluded that the optimized elastic mass attached to the acoustic diaphragm allows flat and smooth frequency response characteristics which can provide the improved sound quality of the piezoelectric acoustic actuator.

References

[1] C. J. Morris and F. K. Forster, "Optimization of a circular piezoelectric bimorph for a micropump driver," *J. Micromech. Microeng.*, vol. 10, pp. 459–465, Sep. 2000.
[2] T. Morita, "Miniature piezoelectric motors," *Sens. Actuators A.*, vol. 103, pp. 291–300, Feb. 2003.
[3] T. Kanda, A. Makino, T. Ono, K. Suzumori, T. Morita, and M. K. Kurosawa, "A micro ultrasonic motor using a micro-machined cylindrical bulk PZT transducer," *Sens. Actuators A.*, vol. 127, pp. 131–138, Feb. 2006.
[4] L. Palm, L. Wallman, T. Laurell, and J. Nilsson, "Development and characterization of silicon micromachined nozzle units for continuous ink jet printers," *J. Imaging Sci. Tech.*, vol. 44, pp. 544–551, Nov. 2000.
[5] H. J. Kim, W. S. Yang, and K. No, "Improvement of low-frequency characteristics of piezoelectric speakers based on acoustic diaphragms," *IEEE Trans. Ultrason. Ferroelectr. Freq. Control*, vol. 59, pp. 2027–2035, Sep. 2012.
[6] S. Yi, S. C. Ur, and E. S. Kim, "Performance of packaged piezoelectric microspeakers depending on the material properties," in *Proc. IEEE 22nd Int. Conf. MEMS*, 2009, pp. 765–768.
[7] K. W. Cho, S. H. Yi, Y. H. Son, and S. Y. Kweon, "Characteristics of pizoelectric micro-speaker fabricated with ZnO thin film," *Integr. Ferroelectr.*, vol. 89, pp. 141–149, Apr. 2007.
[8] H. J. Kim, S. Q. Lee, S. K. Lee, and K. H. Park, "A piezoelectric microspeaker with a high-quality PMN-PT single-crystal membrane," *J. Korean Phys. Soc.*, vol. 54, pp. 930–933, Feb. 2009.
[9] H. J. Kim, K. Koo, S. Q. Lee, K. Park, and J. Kim, "High performance piezoelectric microspeakers and thin speaker array system," *ETRI J.*, vol. 31, pp. 680–687, Dec. 2009.
[10] C. S. Lee, J. Y. Kim, D. E. Lee, J. Joo, S. Han, Y. W. Beag, and S. K. Koh, "An approach to durable poly(vinylidene fluoride) thin film loudspeaker," *J. Mater. Res.*, vol. 18, pp. 2904–2911, Dec. 2003.
[11] T. Horikawa and K. Kobayashi, "Application of ceramic piezoelectric device to audio speaker," in *Proc. SICE Annu. Conf.*, 2008, pp.1–4.
[12] J. H. Kim, S. Yun, J. H. Kim, and J. Kim, "Fabrication of piezoelectric cellulose paper and audio application," *J. Biol. Eng*, vol. 6, pp. 18–21, Mar. 2009.
[13] M. R. Bai and T. Huang, "Development of panel loudspeaker system: Design, evaluation and enhancement," *J. Acoust. Soc. Am.*, vol. 109, pp. 2751–2761, Jun. 2001.
[14] F. Fahy, "Comment on "Development of panel loudspeaker system: Design, evaluation and enhancement," *J. Acoust. Soc. Am.*, vol. 113, pp. 43–44, Jan. 2003.
[15] S. Yuan, S. Huang, X. Chu, and R. Gao, "Optimization methods for acoustic performance of piezoelectric panel loudspeaker," in *Proc.*

Int. Conf. Electronic and Mechanical Engineering and Information Technology, 2011, art no. 6022938, pp. 332–337.
[16] G. Lu and Y. Shen, "Model optimization of orthotropic distributed-mode loudspeaker using attached masses," *J. Acoust. Soc. Am.*, vol. 126, pp. 2294–2300, May 2009.
[17] G. Lu, Y. Shen, and Z. Liu, "Optimization of orthotropic distributed-mode loudspeaker using attached masses and multi-exciters," *J. Acoust. Soc. Am.*, vol. 131, pp. EL93–EL98, Feb. 2012.
[18] Y. H. Huang and C. C. Ma, "Experimental and numerical investigations of vibraion characteristics for parallel-type and series-type triple-layered piezoceramic bimorphs," *IEEE Trans. Ultrason. Ferroelectr. Freq. Control*, vol. 56, pp. 2598–2611, Dec. 2009.
[19] T. Li, Y. H. Chen, and F. Y. C. Boey, "Domain reorientation of piezoelectric bending actuators," *Sens. Actuators A.*, vol. 134, pp. 544–554, Mar. 2007.
[20] Q. M. Wang and L. E. Cross, "Constitutive equations of symmetrical triple layer piezoelectric benders," *IEEE Trans. Ultrason. Ferroelectr. Freq. Control*, vol. 46, pp. 1343–1351, Nov. 1999.
[21] L. K. Chiu, D. V. Anderson, and B. Hoomes, "Audio output enhancement algorithms for piezoelectric loudspeakers," *Proc. IEEE Digital Signal Processing Workshop and IEEE Signal Processing Education Workshop*, 2011, pp. 317–320.
[22] V. V. Varadan, Y. Lim, and V. K. Varadan, "Closed loop finite-element modeling of active/passive damping in structural vibration control," *Smart Mater. Struct.*, vol. 5, pp. 685–694, Oct. 1996.
[23] C. D. Johnson, "Design of passive damping systems," *J. Mech. Des.*, vol. 117(B), pp. 171–176, Jun. 1995.
[24] M. J. Lam, D. J. Inman, and W. R. Saunders, "Vibration control through passive contrained layer damping and active control," *J. Intell. Mater. Syst. Struct.*, vol. 8, pp. 663–677, Aug. 1997.

Hye Jin Kim received the B.S. and M.S. degrees in physics from Chonbuk National University and Seoul National University, Korea, in 1998 and 2001, respectively. She also received the Ph.D. degree in the Department of Material Science and Engineering from the Korea Advanced Institute of Science and Technology (KAIST), Daejeon, Korea, in 2013. Since 2001, she has worked for the Electronics and Telecommunications Research Institute (ETRI) as a senior researcher. Her research interests include piezoelectric materials, sensors and actuators, piezoelectric ceramics, piezoelectric polymers, MEMS microphones, piezoelectric speakers, ultrasonic actuators, and piezoelectric energy harvesters.

Woo Seok Yang received the B.S., M.S., and Ph.D. degrees in materials science and engineering from the Pohang University of Science and Technology, Pohang, Korea, in 1991, 1993, and 1998, respectively. From 1998 to 2001, he worked on FeRAM and DRAM at Hynix Semiconductor Inc. He has been with the Electronics and Telecommunications Research Institute since 2001. His recent research interests are in the fields of physical MEMS devices and USN sensors.

Kwangsoo No received the B.S. degree in ceramic engineering from Hanyang University, Korea, in 1977. He also received the M.S. and Ph.D. degrees in material science and engineering from Iowa State University in 1983 and 1986, respectively. From 1986 to 1988, he was with NASA's Ames Laboratory as a postdoctoral researcher. In 1988, he joined the Department of Material Science and Engineering, Korea Advanced Institute of Science and Technology (KAIST), as a professor. His research interests include ferroelectric and optical thin films, energy harvesting devices, ferroelectric nanostructures, tactile simulators, superconductors, PRAM, and water harvesting.